Chinese Chemical Letters 34 (2023) 108141

Contents lists available at ScienceDirect

Chinese Chemical Letters

journal homepage: www.elsevier.com/locate/cclet

High-throughput quantitative detection of triple-negative breast cancer-associated expressed miRNAs by rolling circle amplification on fluorescence-encoded microspheres

Jieyu Liu[a,1], Liming Zhang[a,1], Wentao Zeng[a], Lihua Zhang[b], Nongyue He[c,d,*], Zhuoxuan Lu[a,*]

[a] Key Laboratory of Tropical Translational Medicine of Ministry of Education, NHC Key Laboratory of Control of Tropical Diseases, School of Tropical Medicine, Micronano Technology Research Institute, School of Basic Medicine and Life Sciences, Hainan Medical University, Haikou 571199, China
[b] Beadstar Biotechnology Hainan Province Co., Ltd., Haikou 570110, China
[c] State Key Laboratory of Bioelectronics, School of Biological Science and Medical Engineering, Southeast University, Nanjing 210096, China
[d] Economical Forest Cultivation and Utilization of 2011 Collaborative Innovation Center in Hunan Province, Hunan Key Laboratory of Biomedical Nanomaterials and Devices, Hunan University of Technology, Zhuzhou 412007, China

ARTICLE INFO

Article history:
Received 28 September 2022
Revised 7 January 2023
Accepted 10 January 2023
Available online 11 January 2023

Keywords:
MicroRNAs
Rolling circle amplification
Fluorescence-encoded microspheres
High-throughput
Triple-negative breast cancer

ABSTRACT

Compared with other types of breast cancer, triple-negative breast cancer (TNBC) has the characteristics of a high degree of malignancy and poor prognosis. Early diagnosis of TNBC through biological markers and timely development of effective treatment methods can reduce its mortality. Many Research experiments have confirmed that some specific miRNA expression profiles in TNBC can used as markers for early diagnosis. However, detecting the expression profiles of multiple groups of miRNAs according to traditional detection methods is complicated and consumes many samples. To address this issue, we developed a method for high-throughput, high-sensitivity quantitative detection of multiple sets of miRNAs (including miR-16, miR-21, miR-92, miR-199, and miR-342) specifically expressed in TNBC by rolling circle amplification (RCA) on fluorescence-encoded microspheres. Through the optimization of reaction system conditions, the developed method showed an extensive linear dynamic range and high sensitivity for all five miRNAs with the lowest limit of detection of 2 fmol/L. Meanwhile, this high-throughput detection method also appeared reasonable specificity. Only in the presence of a specific target miRNA, the fluorescence signal on the correspondingly encoded microspheres is significantly increased, while the fluorescence signal on other non-correspondingly encoded microspheres is almost negligible. Furthermore, this process exhibited good recovery and reproducibility in serum. The advantages of this method allow us to more conveniently obtain the expression profiles of multiple groups of TNBC-associated miRNAs, which is beneficial for the early detection of TNBC.

Triple-negative breast cancer (TNBC) accounts for 15%–20% of women with breast cancer worldwide [1–3]. This subtype of breast cancer has the characteristics of early recurrence and high recurrence rate, so the survival rate of patients with TNBC is meager [2,4]. Finding the biomarkers of TNBC is of great significance for the early diagnosis of TNBC. Different from other breast cancers (the expression levels of estrogen receptor (ER), progesterone receptor (PR), and human epidermal growth factor receptor 2 (HER2)) can provide important reference information for clinicians [5–7], triple-negative breast cancer lacks tumor markers, making early diagnosis extremely difficult. In recent years, studies have proved that some specific miRNA expression profiles in serum can provide important information for the early diagnosis of TNBC [8]. For example, miR-16 [8,9], miR-21 [9–11], miR-92a-3p [9,12], miR-199a-5p [9,13] and miR-342–3p [9,14] were shown to have significant differences in their expression levels between TNBC, non-TNBC and healthy controls. However, simultaneous detection of multiple miRNAs is still a challenging task due to their limited size, low abundance, and complex experimental procedures [15–18].

With the development of micro-nano materials, many pioneering ideas have been opened up for tumor treatment and detection [19–26]. Fluorescence-encoded microspheres, whose unique codes can distinguish different test objects, provide an excellent conve-

* Corresponding authors.
E-mail addresses: nyhe1958@163.com (N. He), Luzhuoxuan1981@163.com (Z. Lu).
[1] These authors contributed equally to this work.

https://doi.org/10.1016/j.cclet.2023.108141
1001-8417/

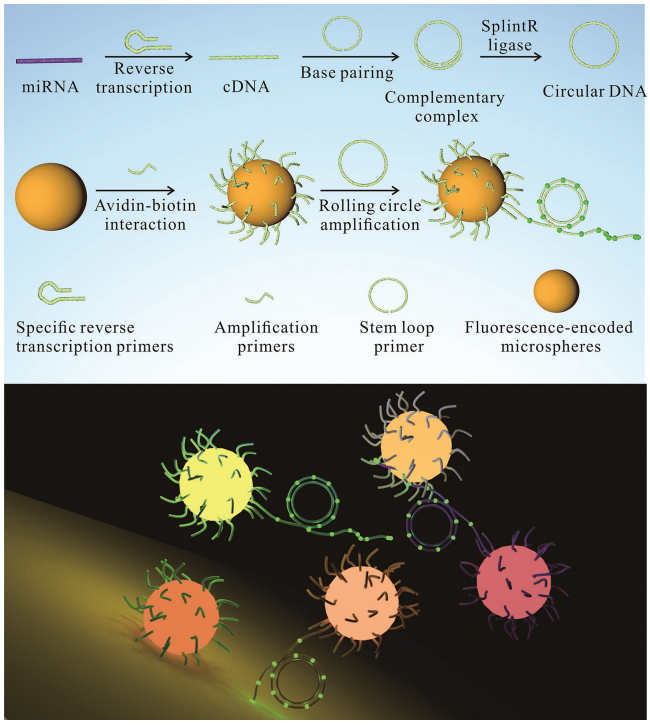

Fig. 1. Schematic illustration of the mechanism of high-throughput quantitative detection of TNBC-associated expressed miRNAs by RCA on fluorescence-encoded microspheres.

nience for high-throughput detection [27–32]. At this stage, some high-throughput detection methods for specific proteins based on fluorescence-encoded microspheres have been developed [33–35], not only for scientific research but also gradually applied to clinical applications, such as the detection of tumor markers [36,37] and cytokines [38,39]. Compared with the high-through detection of protein, the high-through detection methods of nucleic acid (including DNA, RNA and miRNA) based on fluorescence-encoded microspheres are more complicated because a lot of low-abundance nucleic acid fragments need to be amplified before detection [40,41]. While conventional PCR thermal cycling is difficult to perform on the microsphere, this is because the conjugation between the microsphere and the primers is disrupted at high temperatures. Existing detection methods generally perform amplification reactions and then hybridize with probes attached to the microspheres [42,43].

In this study, an assay for high-throughput detection of TNBC-related miRNA expression using rolling circle amplification (RCA) on fluorescence-encoded microspheres was developed. As illustrated in Fig. 1, a specific miRNA is reverse transcribed into cDNA and paired with the corresponding stem-loop primers. Then the stem-loop primers are ligated into a loop under the action of ligase. At the same time, the specific biotinylated capture primers bind to the corresponding specific fluorescence-encoded microspheres. Then these capture primers are complementary to the corresponding specific DNA loops, and the rolling circle process begins under the action of phi29 DNA polymerase. Sequences of all primers can be found in Table S1 (Supporting information). Finally, the encoded fluorescence on the microsphere was detected to identify the analyte to be detected by flow cytometry and calculate the analyte concentration by measuring the fluorescence intensity of the amplified product (iFluor 488-labeled dUTP replaces part of dTTP during amplification) to achieve the purpose of high-throughput quantitative detection.

To establish an RCA system for high-throughput detection of miRNAs on fluorescence-encoded microspheres, the first step is to optimize the RCA system. Initially, we tried to use the miRNA to complement the stem-loop primer and allow it to form a loop under the action of ligases. However, the gel electrophoresis image shows almost no product detected even though three enzymes were used, including T4 DNA ligase, Taq DNA ligase, and SplintR ligase for ligation (Fig. 2A). The possible reason is that miRNAs are so easily degraded that many of them are degraded before the ligation reaction is completed. To ensure that the detection reac-

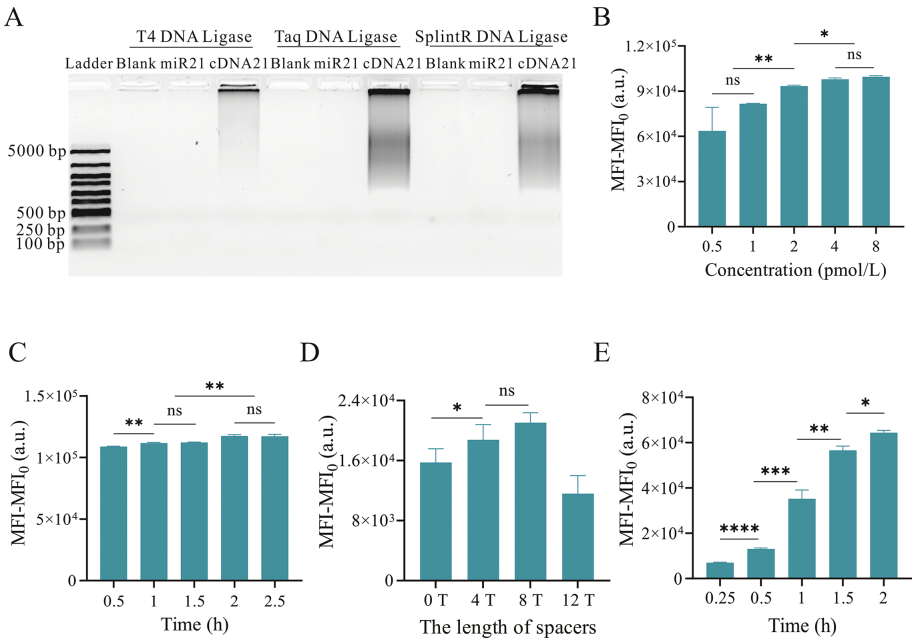

Fig. 2. Optimization of experimental conditions. (A) Agarose gel electrophoresis of RCA products after ligation by T4 DNA ligase, Taq DNA ligase, and SplintR ligase, respectively. (B) Fluorescence intensities of different concentrations of test primers attached to fluorescence-encoded microspheres for 2 h detected by flow cytometry. (C) Fluorescence intensities of the test primers on fluorescence-encoded microspheres after mixing with the microspheres for different times. (D) Fluorescence intensities of amplification products after RCA reaction with amplification primers with different arm lengths. (E) Fluorescence intensities of amplification products for different times of RCA. ns: not significant, $^{*}P < 0.05$, $^{**}P < 0.01$, $^{***}P < 0.001$ and $^{****}P < 0.0001$.

tion is not affected by RNA degradation, we chose to reverse transcribe the miRNA into DNA first and then perform the detection, even though this process was slightly cumbersome. Next, the optimal conditions were explored for attaching extension primers to fluorescence-encoded microspheres. A range of concentrations of 3′ labeled fluorescent and 5′ biotinylated text primers, which are used to directly reflect primer-to-sphere attachment, were mixed with avidinylated fluorescence-encoded microspheres. As shown in Fig. 2B, the fluorescence intensity increases continuously with the increase of primer concentration, and this enhanced trend is not obvious until the primer concentration exceeds 4 pmol/L. Then, we tried to figure out the optimal reaction time for attaching the amplification primers to the microspheres *via* a biotin and avidin system. 3′ labeled fluorescent and 5′ biotinylated test primers were mixed with fluorescence-encoded microspheres for various times. As shown in Fig. 2C, the fluorescence signal continues to increase until the reaction time exceeds 2 h which the fluorescence signal reaches a plateau and no longer increases. Therefore, in the subsequent establishment of the reaction system, these optimized reaction conditions were used to connect the amplification primer on fluorescence-encoded microspheres. Since the amplification primers are attached to the microspheres, steric hindrance occurs when the amplification primers are complementary to the DNA loop [44–46]. A series of amplification primers with different arm lengths were designed to avoid the interference of steric hindrance on amplification efficiency. As illustrated in Fig. 2D, the highest fluorescence values are achieved when the arm is eight bases. Therefore, amplification primers with an 8-base arm were designed in the following experiments. Finally, to determine the time required for the RCA reaction on the microsphere, the fluorescence of amplified products was measured at different amplification times by flow cytometry. As shown in Fig. 2E, with the prolongation of reaction time, the RCA product continues to increase, which is reflected in the fluorescence intensity of iFluor 488-labeled dUTP that enzymatically incorporated into the amplification product. However, excessive reaction products can lead to the aggregation of fluorescence-encoded microspheres. We finally chose 2 h as amplification reaction time to avoid this phenomenon.

Next, the sensitivity of this miRNA detection method was evaluated method. As shown in Fig. 3, the linear detection ranges of 5 TNBC-associated miRNAs (including miR-16, miR-21, miR-92, miR-199, and miR-342) have slightly different (the linear range of miR-16 is 32 fmol/L to 100 pmol/L (Fig. 3A), the linear detection range of miR-21 and miR-199 are 32 fmol/L to 40 pmol/L (Figs. 3B and D), and the linear detection range of miR-92 is 64 fmol/L to 80 pmol/L (Fig. 3C)). The detection range of miR-342 is from 64 fmol/L to 200 pmol/L (Fig. 3E). Among these miRNAs, the lowest limit of detection (LOD, in terms of 3 times deviation over the blank response rule) is calculated as 2 fmol/L (miR-342). The LOD values of miR-199 and miR-92 are also calculated below 10 fmol/L (2.74 and 6.8 fmol/L, respectively). The sensitivity of this assay is comparable to the linear detection range reported in the previous literature [47–50], suggesting that the high-throughput detection method has a wide linear range and a relatively low LOD.

Moreover, the specificity of the method was investigated. As illustrated in Fig. 4, only in the presence of a specific target miRNA, the fluorescent signal on the corresponding encoded microsphere significantly increases. The fluorescence signal on other non-corresponding encoded microspheres is almost negligible. For example, when there is only target miR-21 in the test, the fluorescence intensity detected on the corresponding microsphere is at least 53 times that of other microspheres (Fig. 4B). Furthermore, almost no interfering signal is observed when miR-92, miR-199, and miR-342 are individually tested for specificity as analytes, meaning that no non-specific amplification occurs (Figs. 4C-E). Among the specific detections, the specific detection of miR-16 is the least satisfactory, but its fluorescence intensity on the corresponding encoded microspheres is also at least 6-fold higher than the interference signal (Fig. 4A). According to these results, it can be seen that this method has reasonable specificity, and the cross-linking signal of these five miRNAs is relatively tiny.

To further evaluate the feasibility of the proposed method in practical application, the miR-16, miR-21, miR-92, miR-199, and miR-342 at different concentrations were added to the serum samples. As shown in Table 1, the recovery rates of 5 different concentrations of miRNAs vary from 81.01% to 108.00%, with the relative standard deviation (RSD) less than 8.32%. These results indicate that the developed fluorescence-encoded microspheres-based RCA method can detect multiple miRNAs in complex serum samples.

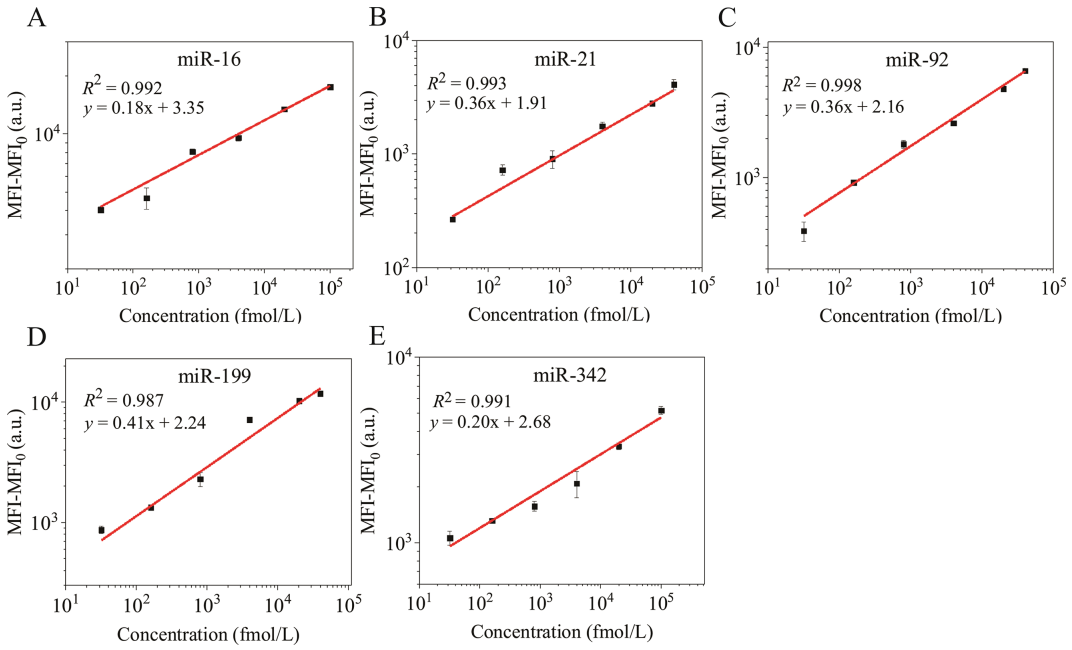

Fig. 3. The linear relationship of (A) miR-16, (B) miR-21, (C) miR-92, (D) miR-199, and (E) miR-342 between mean fluorescence intensity and miRNA concentration.

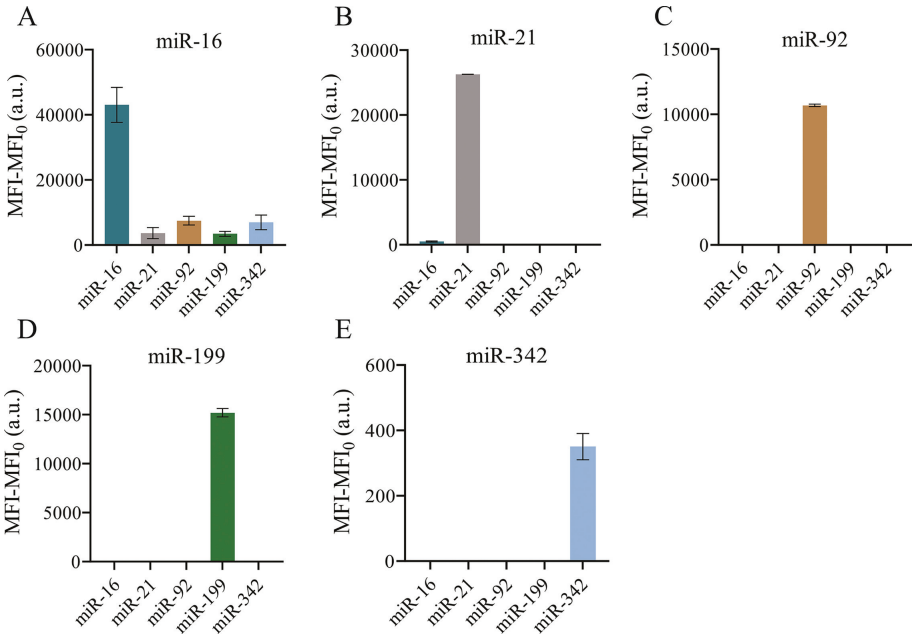

Fig. 4. The selectivity analysis of high-throughput quantitative detection of (A) miR-16, (B) miR-21, (C) miR-92, (D) miR-199 and (E) miR-342 by RCA on fluorescence-encoded microspheres.

Table 1
Recovery data for different concentrations of miR-16, miR-21, miR-92, miR-199, and miR-342 spiked into serum samples.

Sample	Added (pmol/L)	Mean found (pmol/L)	Mean recovery (%)	RSD (%) ($n=3$)
miR-16	0.1	0.098	98.00	2.71
	1	0.886	88.60	6.44
	10	9.177	91.77	3.94
miR-21	0.1	0.108	108.00	3.46
	1	0.855	85.50	4.04
	10	8.101	81.01	3.61
miR-92	0.1	0.107	107.00	3.80
	1	0.854	85.40	3.81
	10	8.959	89.59	3.71
miR-199	0.1	0.101	101.00	8.32
	1	0.957	95.70	0.69
	10	8.248	82.48	0.44
miR-342	0.1	0.096	96.00	1.65
	1	1.042	104.20	2.49
	10	9.228	92.28	5.81

In this study, an RCA-based method was developed for high-throughput quantitative detection of TNBC-associated miRNAs on fluorescence-encoded microspheres. The detection sensitivity was significantly improved by optimizing various conditions, and its dynamic detection range can expand to 3.1 to 3.5 orders of magnitude. Specificity assays showed only a few weak cross-linking signals, indicating very little non-specific amplification. Moreover, we added miRNAs to serum to simulate actual samples and performed concentration detection by the developed method. The data exhibited that the five miRNAs showed good recoveries at three different concentrations. By virtue of these advantages, this high-throughput method for detecting TNBC-associated miRNA expression profiles by isothermal amplification reactions on fluorescence-encoded microspheres has broad potential for clinical application.

Declaration of competing interest

The authors declare that they have no known competing financial interests or personal relationships that could have appeared to influence the work reported in this paper.

Acknowledgments

This work was financially supported by Hainan Provincial Natural Science Foundation of China (No. 822CXTD514), Hainan Province Science and Technology Special Found (No. ZDYF2022SHFZ123).

Supplementary materials

Supplementary material associated with this article can be found, in the online version, at doi:10.1016/j.cclet.2023.108141.

References

[1] T. Wu, L.R. Sultan, J. Tian, et al., Breast Cancer Res. 173 (2019) 365–373.
[2] A. Diana, E. Franzese, S. Centonze, et al., Curr. Oncol. Rep. 20 (2018) 76.
[3] M. Kalimutho, K. Parsons, D. Mittal, et al., Trends Pharmacol. Sci. 36 (2015) 822–846.
[4] N.U. Lin, A. Vanderplas, M.E. Hughes, et al., Cancer 118 (2012) 5463–5472.
[5] R.S. Finn, M.F. Press, J. Dering, et al., Am. J. Clin. Oncol. 27 (2009) 3908–3915.
[6] T. Ishikawa, Y. Ichikawa, D. Shimizu, et al., J. Surg. Sci. 2 (2014) 4–9.
[7] E.A. Rakha, J.S. Reis-Filho, F. Baehner, et al., Breast Cancer Res. 12 (2010) 207.
[8] H. Sabit, E. Cevik, H. Tombuloglu, et al., Crit. Rev. Oncol. Hematol. 157 (2021) 103196.
[9] V.Y. Shin, J.M. Siu, I. Cheuk, et al., Br. J. Cancer 112 (2015) 1751–1759.
[10] T.A. MacKenzie, G.N. Schwartz, H.M. Calderone, et al., Am. J. Pathol. 184 (2014) 3217–3225.
[11] M. Rezayi, Z. Farjami, Z.S. Hosseini, et al., Curr. Pharm. Des. 24 (2018) 4675–4680.
[12] H. Lan, H. Lu, X. Wang, et al., Biomed. Res. Int. 2015 (2015) 125094.
[13] J. Chen, V.Y. Shin, M.T. Siu, et al., BMC Cancer 16 (2016) 887.
[14] T. Ma, J. Zhang, J. Wu, et al., J. Cent. South Univ. 39 (2014) 488–495.
[15] Y. Zhao, X. Fang, M. Bai, et al., Chin. Chem. Lett. 33 (2022) 2101–2104.
[16] Z. Fang, X. Zhang, H. Huang, et al., Chin. Chem. Lett. 33 (2022) 1693–1704.
[17] T. Jet, G. Gines, Y. Rondelez, et al., Chem. Soc. Rev. 50 (2021) 4141–4161.
[18] K. Flatmark, E. Høye, B. Fromm, Scand. J. Clin. Lab. Invest. Suppl. 245 (2016) 80–83.
[19] D. Bannerman, W. Wan, Expert Opin. Drug Deliv. 13 (2016) 1289–1300.
[20] L. Zhang, L. Xu, Y. Wang, et al., Chin. Chem. Lett. 33 (2022) 4089–4095.
[21] Z. Lu, Y. Zhang, Y. Wang, et al., J. Control. Release 332 (2021) 245–259.
[22] L. He, R. Huang, P. Xiao, et al., Chin. Chem. Lett. 32 (2021) 1593–1602.
[23] Z. Cheng, M. Li, R. Dey, et al., J. Hematol. Oncol. 14 (2021) 85.
[24] X. Xu, N. He, Chin. Chem. Lett. 32 (2021) 1747–1750.
[25] D. Kalenichenko, G. Nifontova, A. Karaulov, et al., Nanomaterials (Basel) 11 (2021) 3055.
[26] H. Zhao, E. Su, L. Huang, et al., Chin. Chem. Lett. 33 (2022) 743–746.
[27] Y. Zhao, W. Chen, C. Peng, et al., J. Colloid. Interface Sci. 352 (2010) 337–342.
[28] Y. Li, Y. Wu, C. Luo, et al., J. Mater. 3 (2015) 8262–8271.

[29] W. Kong, C. Xiao, G. Ying, et al., Biosens. Bioelectron. 94 (2017) 420–428.
[30] X. Qu, H. Jin, Y. Liu, et al., Anal. Chem. 90 (2018) 3482–3489.
[31] D. Zhang, T. Xu, E. Chu, et al., PLoS One 16 (2021) e0248444.
[32] K.L. Kellar, M.A. Iannone, Exp. Hematol. 30 (2002) 1227–1237.
[33] R. Wilson, A.R. Cossins, D.G. Spiller, Angew. Chem. Int. Ed. 45 (2006) 6104–6117.
[34] Y.K. Leng, K. Sun, X.Y. Chen, et al., Chem. Soc. Rev. 44 (2015) 5552–5595.
[35] A. Lin, A. Salvador, J.M. Carter, Methods Mol. Biol. 1318 (2015) 107–118.
[36] W.S. Tang, B. Zhang, L.D. Xu, et al., Analyst 147 (2022) 1873–1880.
[37] S.W. Birtwell, G.R. Broder, P.L. Roach, et al., Biomed. Microdevices 14 (2012) 651–657.
[38] V.V. Krishnan, S.R. Selvan, N. Parameswaran, et al., J. Immunol. Methods 461 (2018) 1–14.
[39] S.M. Yang, Q. Lin, H. Zhang, et al., Biosens. Bioelectron. 180 (2021) 113148.
[40] Y.Q. Xiang, H.D. Yan, B.J. Zheng, et al., Anal. Chem. 92 (2020) 12338–12346.
[41] N. Wang, L. Song, T. Deng, et al., Anal. Chim. Acta 1140 (2020) 69–77.
[42] S. Liu, H. Fang, C. Sun, et al., Analyst 143 (2018) 5137–5144.
[43] J.B. Long, Y.X. Liu, Q.F. Cao, et al., Chin. Chem. Lett. 26 (2015) 1031–1035.
[44] M. Zhou, X. Chen, H. Yang, et al., ACS Omega 4 (2019) 6931–6938.
[45] T. Wei, M.N. Pearson, K. Armstrong, et al., Mol. Biosyst. 8 (2012) 1325–1338.
[46] A. Vainrub, B.M. Pettitt, Biopolymers 68 (2003) 265–270.
[47] T. Fan, Y. Mao, Q. Sun, et al., Cancer Sci. 109 (2018) 2897–2906.
[48] S. Gong, J. Li, W. Pan, et al., Anal. Chem. 93 (2021) 10719–10726.
[49] M. Umer, N.B. Aziz, R.G. Mahmudunnabi, et al., Analyst 146 (2021) 5496–5501.
[50] A.A.A. Al-Maskri, G. Jin, Y. Li, et al., Talanta 249 (2022) 123618.